Table III. Selected Bond Distances (Å) and Angles (deg) for (DME)ZrCl$_2$(OSiPh$_3$)$_2$·2C$_6$H$_6$

Zr–Cl	2.464 (7)	Zr–O(1)	1.91 (1)
Zr–O(2)	2.33 (2)	Si–O(1)	1.65 (2)
Si–C(1)	1.86 (3)	Si–C(7)	1.81 (3)
Si–C(13)	1.81 (2)	O(2)–C(19)	1.45 (7)
O(2)–C(20)	1.41 (4)	C(1)–C(2)	1.43 (4)
C(1)–C(6)	1.50 (3)	C(2)–C(3)	1.38 (4)
C(3)–C(4)	1.35 (3)	C(4)–C(5)	1.41 (6)
C(5)–C(6)	1.38 (5)	C(7)–C(8)	1.54 (4)
C(7)–C(12)	1.32 (4)	C(8)–C(9)	1.38 (5)
C(9)–C(10)	1.28 (5)	C(10)–C(11)	1.38 (4)
C(11)–C(12)	1.47 (4)	C(13)–C(14)	1.35 (4)
C(13)–C(18)	1.35 (5)	C(14)–C(15)	1.47 (4)
C(15)–C(16)	1.28 (6)	C(16)–C(17)	1.29 (5)
C(17)–C(18)	1.60 (4)	C(20)–C(20)	1.53 (9)
Cl–Zr–O(1)	95.1 (5)	Cl–Zr–O(2)	83.3 (6)
O(1)–Zr–O(2)	165.8 (8)	O(1)–Si–C(1)	108 (1)
O(1)–Si–C(7)	107.1 (9)	C(1)–Si–C(7)	114 (1)
O(1)–Si–C(13)	109.7 (9)	C(1)–Si–C(13)	109 (1)
C(7)–Si–C(13)	109 (1)	Zr–O(1)–Si	171 (1)
Zr–O(2)–C(19)	127 (2)	Zr–O(2)–C(20)	109 (2)
C(19)–O(2)–C(20)	114 (3)	Si–C(1)–C(2)	123 (1)
Si–C(1)–C(6)	118 (2)	C(2)–C(1)–C(6)	118 (2)
C(1)–C(2)–C(3)	120 (2)	C(2)–C(3)–C(4)	122 (3)
C(3)–C(4)–C(5)	121 (3)	C(4)–C(5)–C(6)	122 (3)
C(1)–C(6)–C(5)	117 (3)	Si–C(7)–C(8)	121 (2)
Si–C(7)–C(12)	125 (2)	C(8)–C(7)–C(12)	114 (3)
C(7)–C(8)–C(9)	118 (3)	C(8)–C(9)–C(10)	123 (3)
C(9)–C(10)–C(11)	123 (4)	C(10)–C(11)–C(12)	116 (3)
C(7)–C(12)–C(11)	125 (3)	Si–C(13)–C(14)	121 (3)
Si–C(13)–C(18)	121 (2)	C(14)–C(13)–C(18)	117 (3)
C(13)–C(14)–C(15)	125 (4)	C(14)–C(15)–C(16)	117 (3)
C(15)–C(16)–C(17)	123 (3)	C(16)–C(17)–C(18)	122 (4)
C(13)–C(18)–C(17)	115 (3)		

single-crystal X-ray structure determination was carried out on **9**.

The structure of the molecule is shown in Figure 2. Table I gives the pertinent crystallographic data for **9**. Fractional co-ordinates for the atoms are listed in Table II. Selected bond distances and angles are given in Table III. There is a distorted-octahedral geometry about the Zr characterized by the Cl–Zr–O(1) angle (95.1 (5)°) and the Cl–Zr–O(2) angle (83.3 (6)°). The molecule lies on a crystallographically required twofold axis, the halves being related by the transformation [−x, y, $^3/_2$ − z]. The bonding interaction between the Zr and the OSiPh$_3$ group is the first siloxy–Zr bond to be structurally characterized. The Zr–O(1) length is short, 1.91 (1) Å, implying some significant d$_\pi$–p$_\pi$ bonding. This is also manifested in the Zr–O(1)–Si bond angle, which is nearly linear, 171 (1)°. These values compare well with zirconium alkoxide linkages in compounds where strong p$_\pi$–d$_\pi$ donation has been claimed: Cp$_2$Zr(O-*t*-Bu)Ru(CO)$_2$Cp (1.910 Å, 169.6°),[10] (Cp$_2$ZrCH$_3$)$_2$O (1.945 Å, 174.1°),[1b] [HB-(3,5-(CH$_3$)$_2$pz)$_3$]Zr(O-*t*-Bu)(η^2-C(CH$_3$)NC(CH$_3$)$_3$) (1.924 Å, 174°),[11] [(*t*-Bu)$_3$CO]ZrCl$_3$·Li(OEt$_2$)$_2$ (1.895 Å (av), 169° (av)).[7] The Zr–O(2) distance, 2.33 (1) Å, is normal and corresponds well with that found for other Zr–O coordinate bonds.[12] Methods to alkylate **9** are currently being explored and will be the subject of a future report.

Supplementary Material Available: Tables of bond distances and angles, final fractional coordinates, and atomic thermal parameters for **9** (4 pages); a table of observed and calculated structure factors for **9** (5 pages). Ordering information is given on any current masthead page.

(10) Casey, C. P.; Jordan, R. F.; Rheingold, A. L. *J. Am. Chem. Soc.* **1983**, *105*, 665.

(11) Reger, D. L.; Tarquini, M. E.; Lebioda, L. *Organometallics* **1983**, *2*, 1763.

(12) Prinz, H.; Bott, S. G.; Atwood, J. L. *J. Am. Chem. Soc.* **1986**, *108*, 2113.

X-ray and Neutron Diffraction Study of the New Cationic Bis(hydrido)-Bridged Platinum–Iridium Complex [(PEt$_3$)$_2$Pt(μ-H)$_2$IrH$_2$(PEt$_3$)$_2$]$^+$[BPh$_4$]$^-$

Alberto Albinati,*[1a] Thomas J. Emge,[1b,d] Thomas F. Koetzle,*[1b] Stefano V. Meille,[1a] Alfredo Musco,[1c,e] and Luigi M. Venanzi*[1c]

The structure of [(PEt$_3$)$_2$Pt(μ-H)$_2$IrH$_2$(PEt$_3$)$_2$]$^+$[BPh$_4$]$^-$ has been studied by X-ray and neutron diffraction techniques, at room temperature and 22 (1) K, respectively. At both temperatures, crystals of the title compound are monoclinic, with space group $P2_1/c$ and $Z = 4$. Unit cell parameters at 22 K are as follows: $a = 18.989$ (10) Å, $b = 15.314$ (3) Å, $c = 19.792$ (6) Å, $\beta = 118.73$ (3)°, and $V = 5047$ (4) Å^3. The coordination around the Ir atom is distorted octahedral, while that around Pt is distorted square planar. The neutron analysis shows that the Pt–Ir distance is 2.677 (1) Å and that the distances between the metals and bridging hydrido ligands differ by 0.15 Å (Ir–H = 1.879 (3) and 1.882 (3) Å; Pt–H = 1.726 (3) and 1.736 (3) Å). The two terminal Ir–H bonds are equivalent (1.586 (3) and 1.591 (3) Å) and comparable in length to those found in other neutron diffraction studies.

Introduction

Bimetallic hydrido-bridged complexes are receiving considerable attention because of their structural features and reactivity, particularly as related to homogeneous catalysis.[2–4]

Among the structural features of interest, mention may be made of (1) the relationship to the formal "donor–acceptor scheme", i.e.

$$L_mMH_2 + (solvent)_2M'L'_n \rightarrow L_mM(\mu\text{-}H)_2M'L'_n + 2\,solvent$$
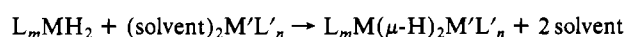
and (2) the influence of direct M–M' interactions.[2]

(1) (a) Universitá di Milano. (b) Brookhaven National Laboratory. (c) ETH, Zürich. (d) Present address: Chemistry Division, Argonne National Laboratory, Argonne, IL 60439. (e) Permanent address: Istituto di Chimica, Facoltá di Scienze, Universitá di Urbino, Urbino, Italy.

(2) Venanzi, L. M. *Coord. Chem. Rev.* **1982**, *43*, 251.

(3) *Ann. N.Y. Acad. Sci.* **1983**, *415*.

(4) Hlatky, G. G.; Crabtree, R. H. *Coord. Chem. Rev.* **1985**, *65*, 1; *Comments Inorg. Chem.* **1985**, *4*, 229.

**Table I.** Crystal Data and Data Collection Parameters for Compound **3**

	X-ray	neutron
formula		$C_{48}H_{84}BIrP_4Pt$
fw		1183.20
data collecn T, K	298	22 (1)
a, Å	19.485 (3)	18.989 (10)
b, Å	15.275 (3)	15.314 (3)
c, Å	20.186 (3)	19.792 (6)
β, deg	118.78 (5)	118.73 (3)
V, Å^3	5264.9 (8)	5047 (4)
Z		4
ρ_{calcd}, g·cm^{-3}	1.492	1.557
space group		$P2_1/c$
cryst dimens, mm	0.2 × 0.3 × 0.4	3.2 × 3.0 × 1.4
radiation λ, Å	0.710 69 (Mo K$\bar{\alpha}$, graphite monochromated)	1.1611 (1) (Ge, 220 reflecting plane)
μ, cm^{-1}	53.6	3.54
transmission factors		
minimum	0.784	0.346
maximum	0.990	0.625
$(\sin \theta)/\lambda$ range, Å^{-1}	0.054–0.572	0.030–0.679
scan mode		$\theta/2\theta$
max scan speed, deg·min^{-1}	6.7	
scan width, deg	1.0 + 0.35 tan θ	2.5 (0.030 Å^{-1} ≤ (sin θ)/λ < 0.431 Å^{-1}), 2.8 (0.431 Å^{-1} ≤ (sin θ)/λ ≤ 0.554 Å^{-1}), 3.5–4.9 (0.554 Å^{-1} ≤ (sin θ)/λ ≤ 0.679 Å^{-1})
max counting time, s	45	
prescan rejection lim	0.5 (2σ)	
prescan acceptance lim	0.025 (40σ)	
bkgd time	0.5 × scan time	
horiz receiving aperture, mm	2.0 + tan θ	12.0
vert receiving aperture, mm	4.0	12.0
measd reflecns	±h,+k,+l	+h,−k,±l; −h,+k,±l
agreement on averaging^a		0.032
no. of data collected	8455	18 639
no. of independent data	8455	13 213
no. of data used in refinements (n_0)	4754 ($|F_o| \geq 3\sigma(F_o)$)	13 213
no. of parameters varied (n_v)	230	1253
R^b	0.033	0.079
$R_w{}^c$	0.035	0.072
goodness of fit (S)^d	1.67	1.15

$^a R_{av} = \sum_i^n |\bar{F}_o^2 - (F_o)_i^2|/\sum_n \bar{F}_o^2$. $^b R$(X-ray) $= \sum ||F_o| - (1/k)|F_c||/\sum |F_o|$; R(neutron) $= \sum |F_o^2 - k^2 F_c^2|/\sum |F_o^2|$. $^c R_w$(X-ray) $= [\sum w(|F_o| - (1/k)|F_c|)^2/\sum w F_o^2]^{1/2}$; R_w(neutron) $= [\sum w(F_o^2 - k^2 F_c^2)^2/\sum w F_o^4]^{1/2}$. $^d S$(X-ray) $= [\sum w(|F_o| - (1/k)|F_c|)^2/(n_o - n_v)]^{1/2}$; S(neutron) $= [\sum w(F_o^2 - k^2 F_c^2)^2/(n_o - n_v)]^{1/2}$.

It is noteworthy that a recently described hydrogenation catalyst has been assigned the hydrido-bridged structure[5]

1
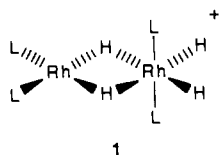
Recent work has shown that bis(hydrido)-bridged species of the type $[L(R)Pt(\mu\text{-}H)_2IrHL_3]^+$ (**2**) (R = H, carbyl; L = tertiary

2   **2'**
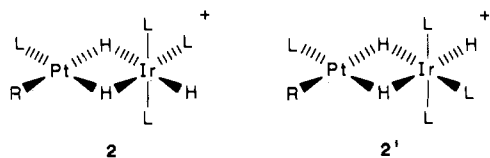
phosphine) are obtained readily from *trans*-$[PtR(solvent)L_2]^+$ and $[IrH_5L_2]$.[6] Compounds **2a,b** (L = PEt$_3$; R = H and Et, respectively) react with H$_2$ to give complex **3**, which is isomeric with

3
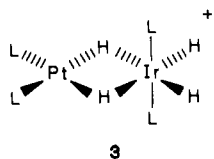
2a and **2'a** and isolobal with **1**. An X-ray investigation of compounds **2'b** and **2c**[7] (L = PEt$_3$; R = Et and Ph, respectively) has shown that the locations of the non-hydride ligands are such as to indicate that the Pt–Ir bridges may not be symmetrical. This assymmetry may arise from the different trans influences of the L and R ligands on Pt, on the one hand, and of the L and H equatorial ligands on Ir, on the other. It was thus thought to be informative to analyze the crystal structure of **3** by neutron diffraction methods, in order to locate the bridging H atoms and to allow a discussion of bridge formation by the "donor–acceptor scheme" as well as to obtain an estimate of mutual trans influences.

Experimental Section

Yellow air-stable crystals of compound **3** (L = PEt$_3$) were prepared as described previously,[6] by slow evaporation from an acetone/methanol solution as the [BPh$_4$]$^-$ salt.

X-ray Diffraction. A suitable crystal of prismatic habit was chosen for the data collection and mounted on a glass fiber in an arbitrary orientation.

An Enraf-Nonius CAD4 automated diffractometer was used both for the determination of the lattice parameters and for data collection. From systematic absences the space group was determined unambiguously to be $P2_1/c$. Crystal data and experimental parameters are summarized in Table I.

The cell parameters were obtained by a least-squares fit of the 2θ values of 25 higher order reflections (0.244 Å^{-1} ≤ (sin θ)/λ ≤ 0.364 Å^{-1}) with the centering routines installed on the CAD4/SDP system.[8] A group of three standard reflections ($\bar{4},\bar{1},10$; $6,\bar{1},\overline{10}$; 545) were measured

(5) Muetterties, E. L.; Burch, R. R.; Stolzenberg, A. M. *Annu. Rev. Phys. Chem.* **1982**, *33*, 89. Meier, E. B.; Burch, R. R.; Muetterties, E. L.; Day, V. W. *J. Am. Chem. Soc.* **1982**, *104*, 2661.

(6) Boron, P.; Musco, A.; Venanzi, L. M. *Inorg. Chem.* **1982**, *21*, 4192.

(7) Immirzi, A.; Porzio, W.; Bachechi, F.; Zambonelli, L.; Venanzi, L. M. *Gazz. Chim. Ital.* **1983**, *113*, 537.

(8) Enraf-Nonius Structure Determination Package, SDP; Enraf-Nonius: Delft, The Netherlands, 1980.

every 130 min to check the stability of the experimental conditions and of the crystal; no significant intensity variation was detected. A set of three reflections ($23\bar{7}$; $6,\bar{1},\overline{10}$; $2,\bar{2},\overline{11}$) was centered after every 250 measurements to check the crystal orientation.

The empirical absorption correction was based on azimuthal (ψ) scans of three reflections with $\chi \geq 81°$: $\bar{2}\,\bar{4}\,0$; $\bar{4}\,\bar{8}\,0$; $\bar{6},\overline{11},\bar{1}$. The SDP system of programs was used for both absorption correction and data reduction.

Structure factors were calculated in the usual way (Lp corrections applied), and the standard deviations on intensities were calculated in terms of counting statistics. Only those reflections with $|F_o| \geq 3\sigma(F_o)$ were used for the solution and refinement of the structure.

The structure was solved by standard Patterson and Fourier methods and refined by blocked-matrix least squares with use of the SHELX program[9] (the function minimized is $\sum w(|F_o| - (1/k)|F_c|)^2$) with weights expressed as $w = a[\sigma^2(F) + bF^2]^{-1}$ (values of the refined parameters are $a = 1.4744$ and $b = 0.000389$).

The phenyl rings of the tetraphenylborate anion were constrained to have idealized D_{6h} geometry (C–C = 1.395 Å and C–C–C = 120.0°). Anisotropic temperature factors were used for Pt, Ir, P, and B atoms and isotropic factors for the others. The contribution of the organic H atoms, placed at their idealized positions (C–H = 1.08 Å), was taken into account, but these atoms were not refined. No extinction correction was deemed necessary. A correction for the real part of the anomalous dispersion was included.[10]

Upon convergence, a difference Fourier synthesis revealed four peaks that could be assigned to the terminal and bridging hydrides. The peaks persisted in a difference synthesis calculated with a limited data set ((sin θ)/λ cutoff 0.33 Å^{-1}),[11] and accordingly these H atoms were included in the last cycles of refinement. Only the bridging hydrides refined satisfactorily (M–H in the range 1.7–2.0 Å). The terminal hydrides refined to give unreasonable bond distances and were omitted from the final model.

The final agreement factors are shown in Table I. A complete list of the positional and thermal parameters (Table S1) and a compilation of observed and calculated structure factors (Table S2) are given in the supplementary material.

Neutron Diffraction. A tablet-shaped crystal with a volume of 14 mm^3 and weight of 21 mg was mounted on an Al pin approximately along the crystallographic $21\bar{1}$ axis. The mount was sealed under a He atmosphere in an Al can attached to a closed-cycle He refrigerator,[12] which was placed on a four-circle diffractometer[13,14] at the Brookhaven High Flux Beam Reactor. The sample was cooled to 22 (1) K from room temperature at a rate of 1–2 deg·min^{-1} and remained at this temperature throughout data collection. Calibration of the Ge-monochromated neutron beam was carried out with a KBr crystal (a_0) = 6.6000 (1) Å at 298 K),[15] yielding a wavelength of 1.1611 (1) Å. A least-squares fit of the sin^2 θ values of 32 centered reflections (16 Friedel pairs in the range 0.377 Å^{-1} < (sin θ)/λ < 0.457 Å^{-1}) gave unit-cell parameters listed in Table I.

Intensity data were collected in the $\theta/2\theta$ step-scan mode. The $+h,-k,\pm l$ quadrant of reciprocal space was scanned, plus the symmetry-related $-h,+k,\pm l$ quadrant for the low-angle region (0.030 Å^{-1} < (sin θ)/λ < 0.463 Å^{-1}). The variable scans for the high-angle region (0.554 Å^{-1} < (sin θ)/λ < 0.679 Å^{-1}) were determined by the dispersion relation:

$$\Delta 2\theta \ (\text{deg}) = 1.10 + 2.97 \tan \theta$$

The total width of any scan was adjusted to give between 60 and 100 steps, which allowed at least one-fourth of each scan for left and right background. The duration of each scan step was about 2 s and depended on a constant monitor count of the incident beam. Three reference intensities were measured after every 100 reflections and showed no significant variation throughout the course of the experiment.

Backgrounds were computed on the basis of the counts recorded for seven steps at either end of each scan, and the resulting integrated intensities were then corrected for Lorentz and absorption effects. The latter correction employed a numerical integration over a Gaussian grid of 10 × 8 × 10 points relative to the reciprocal cell vectors. Averaging of identical or symmetry-related data yielded 13 213 unique squared structure factors, all of which were used in the structure refinement.

Starting values for the coordinates of non-hydrogen atoms were taken from the X-ray results. These coordinates initially were refined together with isotropic temperature factors by means of a differential-synthesis technique. After location of all H atoms on difference maps the differential synthesis refinement was resumed, varying positional and anisotropic thermal parameters for all 139 atoms. The final cycles of refinement were completed by means of a least-squares procedure, with blocks of up to 443 variable parameters. A type I isotropic extinction correction[16] was included in the model. The most significant extinction corrections were for reflections along the $10\bar{1}$ vector (e.g., factors 0.82 dividing F_o^2 for $40\bar{4}$ and 0.83 for $20\bar{2}$).

The quantity $\sum w(F_o^2 - k^2 F_c^2)^2$, with weights $w = [\sigma^2(F_o^2)]^{-1}$ for $\sigma^2(F_o^2) = [\sigma_{count}^2(F_o^2) + (0.02F_o^2)^2]$, was minimized in the least-squares procedure, at the completion of which all atomic positional parameter shift/error values were 0.1 or less. The final difference-Fourier synthesis produced no significant structural features. Indices of fit are presented in Table I. Final atomic positional and equivalent isotropic thermal parameters are listed in Table II. Tables of anisotropic thermal parameters (Table S3) and observed and calculated squared structure factors and esd's (Table S4), an extensive list of bond distances and angles (Table S5), and a view of the [BPh$_4$]$^-$ anion (Figure S1) are provided as supplementary material.

Neutron scattering lengths were taken from a compilation of Koester.[17] Computer programs employed include DIFSYN (a differential synthesis refinement),[18] a modified version of the full-matrix least-squares program UPALS,[19] the absorption procedure of Coppens, Leiserowitz, and Rabinovich,[20] C. K. Johnson's ORTEP,[21] and locally written programs.

Results and Discussion

A view of the cation **3** is given in Figure 1, and Table III lists bond distances and angles from the X-ray and neutron diffraction analyses. Bonding parameters for a number of related bimetallic hydrido-bridged complexes are compared in Table IV.

There are very few significant differences between the X-ray and neutron models for **3**. The very slightly shorter metal–metal separation at 22 K ($\Delta = 0.008$ (2) Å) may possibly be due to the difference in temperature of the two experiments. This effect has already been observed in a study of the [H$_3$Pt$_2$(diphos)$_2$]$^+$ (**4**) cation.[31]

As expected, the H atom positions from X-ray diffraction are relatively poorly determined. The results of the neutron analysis

(9) Sheldrick, G. M. SHELX Programs; University of Cambridge: Cambridge, England.

(10) *International Tables for X-ray Crystallography*; Kynoch: Birmingham, England, 1974; Vol. IV.

(11) LaPlaca, S. J.; Ibers, J. A. *Acta Crystallogr.* **1965**, *18*, 511.

(12) Air Products and Chemicals, Inc., DISPLEX Model CS-202.

(13) McMullan, R. K.; Andrews, L. C.; Koetzle, T. F.; Reidinger, F.; Thomas, R.; Williams, G. J. B. "NEXDAS, Neutron and X-ray Data Acquisition System", unpublished work.

(14) Dimmler, D. G.; Greenlaw, N.; Kelley, M. A.; Potter, D. W.; Rankowitz, S.; Stubblefield, F. W. *IEEE Trans. Nucl. Sci.* **1976**, *NS-23*, 298.

(15) Donnay, J. D. H.; Ondik, H. M., Eds. *Crystal Data Determinative Tables*, 3rd ed.; U.S. Department of Commerce and Joint Committee on Powder Diffraction Standards: Washington, DC, 1973; Vol. 2, p C-164.

(16) Becker, P. J.; Coppens, P. *Acta Crystallogr., Sect. A: Cryst. Phys., Diffr., Theor. Gen. Crystallogr.* **1975**, *A31*, 417.

(17) Koester, L. In *Neutron Physics*; Springer-Verlag: Berlin, Heidelberg, New York, 1977; p 36.

(18) McMullan, R. K., unpublished work.

(19) Lundgren, J.-O. "Crystallographic Computer Programs"; Report UUIC-B13-4-05; Institute of Chemistry, University of Uppsala: Uppsala, Sweden, 1982.

(20) Coppens, P.; Leiserowitz, L. L.; Rabinovich, D. *Acta Crystallogr.* **1965**, *18*, 1035.

(21) Johnson, C. K. *Oak Ridge Natl. Lab.*, [*Rep.*] ORNL (*U.S.*) **1976**, ORNL-5138.

(22) Musco, A.; Naegeli, R.; Venanzi, L. M.; Albinati, A. *J. Organomet. Chem.* **1982**, *228*, C15.

(23) Albinati, A.; Lehner, H.; Venanzi, L. M. *Inorg. Chem.* **1985**, *24*, 1483.

(24) Robertson, G. B.; Tucker, P. A. *Aust. J. Chem.* **1984**, *37*, 257.

(25) Wei, C.-Y.; Marks, M. W.; Bau, R.; Kirtley, S. W; Bisson, D. E.; Henderson, M. E.; Koetzle, T. F. *Inorg. Chem.* **1982**, *21*, 2556.

(26) Alcock, N. W.; Howarth, O. S.; Moore, P.; Morris, G. E. *J. Chem. Soc., Chem. Commun.* **1979**, 1160.

(27) Albinati, A.; Naegeli, R.; Togni, A.; Venanzi, L. M. *Organometallics* **1983**, *2*, 926.

(28) Teller, R. G.; Williams, J. M.; Koetzle, T. F.; Burch, R. R.; Gavin, R. M.; Muetterties, E. L. *Inorg. Chem.* **1981**, *20*, 1806.

(29) Barnett, B. L.; Krüger, C.; Tsay, Y. H.; Summerville, R. H.; Hoffmann, R. *Chem. Ber.* **1977**, *110*, 3990.

(30) Bachechi, F.; Bracher, G.; Grove, D. M.; Kellenberger, B.; Pregosin, P. S.; Venanzi, L. M.; Zambonelli, L. *Inorg. Chem.* **1983**, *22*, 1031.

(31) Chiang, M. Y.; Bau, R.; Minghetti, G.; Bandini, A. L.; Banditelli, G.; Koetzle, T. F. *Inorg. Chem.* **1984**, *23*, 122.

Table II. Atomic Parameters for Compound 3 from the Neutron Diffraction Study at 22 K[a]

atom	x	y	z	U_{iso}	atom	x	y	z	U_{iso}
Ir	14660 (4)	18009 (5)	17920 (4)	72 (2)	H33B	28515 (17)	−439 (20)	−5041 (16)	279 (10)
Pt	24550 (4)	15217 (5)	12041 (4)	36 (2)	H34A	38002 (23)	−9742 (25)	6373 (22)	488 (16)
P1	8522 (9)	30155 (10)	10616 (8)	75 (5)	H34B	28112 (22)	−11109 (23)	4165 (24)	522 (16)
P2	19212 (8)	6353 (10)	26257 (9)	72 (5)	H34C	34383 (21)	−4652 (22)	12073 (17)	376 (13)
P3	22714 (8)	8220 (10)	1167 (9)	83 (5)	H35A	9026 (16)	5100 (22)	−2589 (18)	327 (12)
P4	37478 (8)	19397 (10)	16158 (8)	58 (4)	H35B	15404 (18)	−3731 (20)	2327 (17)	317 (12)
HB1	25016 (15)	21017 (19)	19726 (15)	235 (10)	H36A	6251 (19)	−7713 (23)	−11572 (20)	404 (13)
HB2	14787 (15)	12240 (20)	9585 (15)	251 (10)	H36B	16228 (20)	−7831 (26)	−9776 (22)	479 (15)
HT1	6012 (15)	15613 (20)	16730 (17)	276 (10)	H36C	9944 (21)	981 (23)	−14618 (17)	397 (13)
HT2	14380 (17)	22913 (19)	24873 (15)	246 (10)	H41A	37761 (17)	22159 (18)	4355 (15)	244 (10)
C11	2171 (7)	36442 (8)	13504 (7)	90 (4)	H41B	46018 (14)	26922 (19)	12240 (16)	243 (10)
C12	6415 (7)	40632 (8)	21475 (7)	122 (4)	H42A	37033 (19)	38766 (20)	4237 (19)	334 (13)
C13	1018 (7)	27791 (9)	600 (7)	129 (4)	H42B	36608 (22)	38601 (20)	12876 (18)	369 (13)
C14	−4843 (7)	20585 (9)	−13 (8)	166 (5)	H42C	28661 (17)	34075 (22)	4454 (21)	375 (13)
C15	15275 (7)	38225 (8)	9920 (7)	112 (4)	H43A	50871 (14)	13959 (18)	20855 (16)	241 (10)
C16	11526 (8)	46528 (9)	5243 (8)	158 (5)	H43B	43757 (17)	6964 (17)	13819 (16)	241 (10)
C21	18318 (7)	−4665 (8)	22263 (7)	131 (4)	H44A	49635 (18)	−505 (20)	26469 (19)	328 (12)
C22	9589 (9)	−7646 (10)	17427 (9)	210 (5)	H44B	39426 (16)	1872 (21)	23594 (17)	300 (11)
C23	14171 (7)	5414 (8)	32133 (7)	105 (4)	H44C	47143 (18)	8292 (20)	30639 (16)	310 (11)
C24	17060 (7)	−1892 (9)	38141 (7)	133 (4)	H45A	40029 (16)	21979 (19)	28951 (15)	237 (10)
C25	29883 (7)	6902 (8)	33366 (7)	107 (4)	H45B	36766 (16)	31480 (18)	23454 (17)	252 (10)
C26	32047 (7)	15441 (9)	37923 (7)	142 (4)	H46A	50903 (17)	33420 (21)	33439 (17)	329 (11)
C31	20389 (7)	15651 (9)	−6949 (7)	114 (4)	H46B	50761 (18)	33134 (22)	24465 (18)	332 (12)
C32	13188 (8)	21619 (9)	−9055 (8)	144 (4)	H46C	54070 (16)	23977 (20)	30543 (19)	330 (11)
C33	30618 (7)	1589 (8)	942 (7)	112 (4)	B	30872 (8)	65814 (9)	29269 (8)	57 (4)
C34	32945 (8)	−6396 (9)	6221 (8)	159 (4)	C1′	33719 (6)	55986 (7)	33028 (7)	71 (3)
C35	13981 (7)	998 (9)	−2313 (7)	124 (4)	C2′	28288 (7)	48935 (8)	30372 (7)	89 (4)
C36	11511 (8)	−3632 (9)	−9967 (8)	174 (4)	C3′	30586 (7)	40330 (8)	32830 (7)	88 (4)
C41	39474 (7)	26013 (8)	9581 (7)	80 (4)	C4′	38542 (7)	38473 (8)	38258 (7)	91 (4)
C42	35189 (7)	34846 (8)	7677 (7)	128 (4)	C5′	44093 (7)	45287 (8)	41008 (7)	93 (4)
C43	44973 (7)	10764 (8)	18962 (7)	81 (4)	C6′	41691 (6)	53821 (8)	38362 (7)	75 (3)
C44	45273 (7)	4780 (8)	25271 (7)	114 (4)	C7′	21743 (6)	67881 (8)	28062 (7)	76 (3)
C45	40985 (7)	26019 (8)	24881 (7)	80 (4)	C8′	14728 (6)	64970 (8)	21550 (7)	88 (4)
C46	49669 (7)	29285 (9)	28499 (7)	118 (4)	C9′	7032 (7)	66313 (8)	20678 (7)	106 (4)
H11A	−2356 (16)	31822 (20)	13186 (17)	278 (11)	C10′	6044 (7)	70784 (8)	26298 (7)	103 (4)
H11B	−1002 (16)	41404 (19)	9056 (16)	269 (10)	C11′	12857 (7)	73886 (8)	32736 (7)	112 (4)
H12A	2033 (18)	43498 (23)	22903 (18)	355 (12)	C12′	20506 (7)	72448 (8)	33575 (7)	95 (4)
H12B	10395 (19)	45858 (22)	21750 (20)	388 (14)	C13′	30504 (6)	65829 (8)	20779 (6)	74 (3)
H12C	9842 (21)	35815 (21)	25833 (17)	384 (12)	C14′	34178 (7)	59333 (8)	18464 (7)	83 (4)
H13A	4201 (17)	25836 (23)	−2540 (16)	316 (11)	C15′	33770 (7)	59354 (8)	11180 (7)	98 (4)
H13B	−2277 (18)	33832 (21)	−2053 (16)	320 (11)	C16′	29486 (7)	65833 (8)	5828 (7)	107 (4)
H14A	−9729 (18)	20069 (25)	−5909 (18)	395 (12)	C17′	25647 (7)	72276 (8)	7871 (7)	106 (4)
H14B	−7561 (19)	21888 (25)	3641 (19)	387 (13)	C18′	26226 (7)	72275 (8)	15181 (7)	94 (4)
H14C	−1806 (19)	14282 (21)	1707 (20)	374 (13)	C19′	36899 (6)	73414 (8)	35093 (7)	71 (3)
H15A	18664 (17)	34623 (20)	7651 (18)	306 (12)	C20′	39956 (7)	72812 (8)	43157 (7)	89 (4)
H15B	19706 (16)	39898 (20)	15918 (16)	280 (10)	C21′	44331 (7)	79518 (8)	48240 (7)	100 (4)
H16A	16185 (18)	50921 (21)	5452 (20)	374 (13)	C22′	45940 (7)	87210 (8)	45405 (7)	105 (4)
H16B	8122 (19)	50120 (21)	7457 (20)	364 (14)	C23′	43086 (7)	88021 (8)	37504 (7)	100 (4)
H16C	7464 (20)	44971 (23)	−849 (18)	396 (13)	C24′	38677 (7)	81243 (8)	32482 (7)	84 (4)
H21A	21696 (19)	−9279 (19)	27005 (17)	309 (11)	H2′	22059 (14)	50257 (18)	26189 (17)	261 (10)
H21B	21348 (18)	−4497 (21)	18705 (17)	312 (12)	H3′	26178 (15)	35051 (17)	30495 (16)	237 (10)
H22A	9319 (22)	−14376 (23)	15539 (22)	462 (16)	H4′	40430 (16)	31843 (17)	40321 (17)	252 (10)
H22B	6367 (21)	−3458 (27)	12382 (20)	469 (14)	H5′	50324 (14)	43943 (18)	45255 (16)	250 (10)
H22C	6389 (20)	−7528 (26)	20761 (21)	437 (14)	H6′	46198 (14)	58977 (18)	40577 (15)	224 (9)
H23A	7702 (15)	4848 (21)	28070 (17)	286 (11)	H8′	15251 (15)	61554 (20)	17007 (15)	257 (10)
H23B	14877 (18)	11779 (18)	34863 (17)	282 (12)	H9′	1736 (15)	63828 (21)	15506 (16)	283 (10)
H24A	13483 (20)	−2116 (23)	41120 (9)	367 (13)	H10′	94 (15)	71711 (20)	25749 (17)	265 (10)
H24B	23277 (18)	−947 (24)	42568 (19)	397 (12)	H11′	12361 (16)	77361 (20)	37280 (17)	281 (10)
H24C	16621 (24)	−8276 (20)	35601 (20)	416 (15)	H12′	25680 (15)	75041 (20)	38711 (15)	254 (10)
H25A	33142 (16)	6339 (21)	30030 (17)	293 (11)	H14′	37401 (16)	54085 (17)	22466 (15)	222 (10)
H25B	31541 (16)	1177 (18)	37163 (16)	257 (10)	H15′	36759 (17)	54242 (19)	9690 (6)	265 (11)
H26A	38431 (17)	15784 (23)	42007 (18)	375 (11)	H16′	29127 (17)	65855 (21)	176 (17)	284 (11)
H26B	28773 (19)	16121 (23)	41183 (18)	358 (13)	H17′	22147 (16)	77265 (19)	3708 (16)	263 (10)
H26C	30471 (19)	21040 (19)	34053 (18)	338 (12)	H18′	23083 (16)	77354 (18)	16569 (15)	242 (10)
H31A	19514 (17)	11509 (20)	−11801 (16)	281 (11)	H20′	38697 (16)	66966 (17)	45519 (15)	237 (10)
H31B	25821 (16)	19461 (19)	−5459 (17)	272 (10)	H21′	46397 (17)	78788 (19)	54383 (15)	265 (10)
H32A	11929 (19)	25374 (21)	−14171 (17)	342 (12)	H22′	49333 (17)	92485 (18)	49323 (17)	265 (10)
H32B	14375 (19)	26105 (21)	−4379 (18)	347 (12)	H23′	44300 (17)	93930 (18)	35238 (17)	262 (11)
H32C	7805 (17)	17897 (21)	−10326 (19)	347 (12)	H24′	36511 (16)	82128 (19)	26272 (15)	248 (10)
H33A	35755 (15)	5876 (19)	2368 (17)	269 (11)					

[a] Positional parameters ×10⁵ and equivalent isotropic thermal parameters ($Å^2$) ×10⁴.

are used in the following discussion.

The structure of **3** may be described as comprising a distorted-square-planar Pt(II) center and a distorted-octahedral *mer*-[IrH₄(PEt₃)₂] unit sharing two bridging hydrido ligands. The [P₂Pt(μ-H)₂IrH₂P₂] core exhibits approximate C_{2v} symmetry. The short Pt–Ir separation of 2.677 (1) Å in this compound is indicative of significant metal–metal interaction (the sum of the atomic radii is 2.744 Å[32]) and is comparable with the Rh–Ir distance of 2.662

Table III. Bond Distances (Å) and Angles (deg) in the [(PEt₃)₂Pt(μ-H)₂IrH₂(PEt₃)₂]⁺ Cation (3)

	X-ray	neutron		X-ray	neutron
Ir–Pt	2.685 (1)	2.677 (1)	Ir–HT1		1.586 (3)
Ir–HB1	1.70 (10)	1.879 (3)	Ir–HT2		1.591 (3)
Ir–HB2	2.05 (10)	1.882 (3)			
Pt–HB1	1.67 (10)	1.726 (3)	Pt–HB2	1.53 (8)	1.736 (3)
HT1–HT2		1.977 (4)	HB1–HB2		2.421 (4)
Ir–P1	2.300 (2)	2.300 (2)	Pt–P3	2.274 (3)	2.276 (2)
Ir–P2	2.293 (2)	2.299 (2)	Pt–P4	2.276 (3)	2.275 (2)
P1–C11	1.846 (14)	1.836 (12)	P3–C31	1.863 (12)	1.841 (2)
P1–C13	1.822 (11)	1.837 (2)	P3–C33	1.822 (14)	1.830 (2)
P1–C15	1.835 (12)	1.833 (2)	P3–C35	1.804 (12)	1.830 (2)
P2–C21	1.820 (15)	1.836 (2)	P4–C41	1.822 (14)	1.827 (2)
P2–C23	1.830((15)	1.833 (2)	P4–C43	1.833 (11)	1.823 (2)
P2–C25	1.848 (11)	1.831 (2)	P4–C45	1.801 (11)	1.830 (2)
C–C$_{av}$ (ethyl)^a	1.515 (38)	1.529 (2)	C–H$_{av}$ (methylene)	1.08^b	1.099 (5)^a
C–H$_{av}$ (methyl)	1.08^b	1.089 (5)^a			
Ir–HB1–Pt	105.5 (4.0)	95.77 (12)	HB1–Ir–P2	92.1 (2.8)	93.20 (10)
Ir–HB2–Pt	96.1 (3.7)	95.35 (13)	HB2–Ir–P2	98.9 (2.2)	96.08 (11)
HT1–Ir–HT2		76.99 (15)	HB1–Ir–HB2	71.2 (3.9)	80.13 (12)
HT1–Ir–HB1		177.70 (14)	HB1–Pt–HB2	87.0 (4.7)	88.70 (13)
HT2–Ir–HB2		178.95 (14)	HB1–Pt–P4	93.0 (3.1)	87.14 (10)
HT1–Ir–HB2		102.12 (14)	HB2–Pt–P3	82.2 (3.7)	87.36 (10)
HT2–Ir–HB1		100.76 (14)	HB1–Pt–P3	169.2 (3.1)	174.23 (10)
HB1–Ir–P1	96.7 (2.8)	95.11 (10)	HB2–Pt–P4	173.9 (3.0)	175.65 (10)
HB2–Ir–P1	90.2 (2.1)	92.57 (11)			
P1–Ir–P2	168.9 (1)	168.91 (6)	Pt–Ir–Pt	94.8 (1)	95.03 (2)
P3–Pt–P4	97.8 (1)	96.87 (6)	Ir–Pt–P3	131.5 (1)	131.73 (5)
Pt–Ir–P1	96.3 (1)	96.05 (5)	Ir–Pt–P4	130.7 (1)	131.38 (6)
Ir–P–C$_{av}$^{a}	115.1 (2.1)	115.3 (2.0)	P–C–C$_{av}$^{a}	114.0 (2.2)	114.7 (1.9)
Pt–P–C$_{av}$^{a}	115.0 (4.3)	114.8 (4.8)	C–P–C$_{av}$^{a}	103.4 (2.6)	103.3 (2.0)

^{a} Mean value; the esd on the mean is estimated from the formula $\sigma(\bar{x}) = [\sum(x_i - \bar{x})^2/n(n-1)]^{1/2}$, where $\bar{x}$ is the mean value and n is the number of observations. ^{b} Value held fixed during refinement.
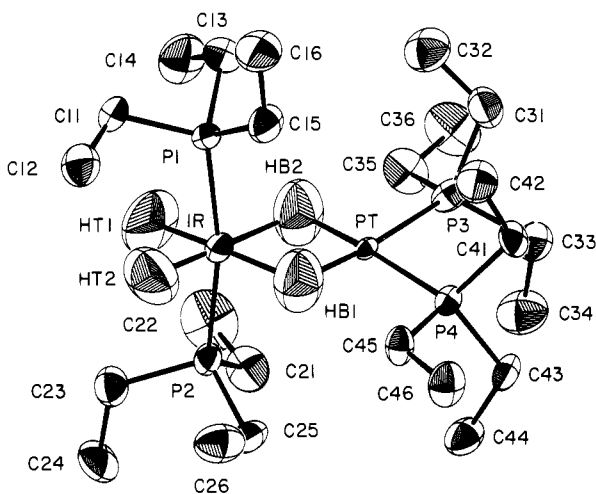
Figure 1. View of the [(PEt₃)₂Pt(μ-H)₂IrH₂(PEt₃)₂]⁺ cation (3) with thermal ellipsoids drawn to include 25% probability.[21]

(1) Å found in compound **5**.[22] On the other hand, longer metal–metal distances indicative of weaker interactions are found in the range 2.7–3.0 Å, as in the case of compounds **6–9** (see Table IV). The extent of the metal–metal interaction in **3** is also reflected in the M–H–M angle (mean value 95.5 (1)°),[25,33–35] comparable to that of 94.1 (4)° found in **11** but smaller, as expected, than the value of 102.7 (1)° found in **8**, where a long W–W separation is present. As already noted in other compounds (**8** and **11**), the bridging H ligands are displaced from the idealized position, i.e., the intersection of the H$_t$–Ir and P–Pt vectors.[25,28,36]

The present analysis provides the first precise determination of the M–H distances bridging two different metal centers. As expected, there is a significant difference between the Ir–H$_b$ and Pt–H$_b$ distances, caused by the different electronic situation of the two metal centers. The two Pt–H$_b$ distances are equivalent (average 1.731 (5) Å) and are longer than those found in **4** involving the square-planar Pt center (1.656 (2) and 1.691 (2) Å) but significantly shorter than the Ir–H$_b$ bonds (average 1.881 (5) Å). This difference may be ascribed to the strong trans influence of the terminal hydrido ligands on iridium.

The terminal Ir–H bond distances (average 1.589 (3) Å) may be compared to those found in IrH₅(P(i-Pr)₃)₂ (**14**) (average 1.603 (9) Å)[37] and C₅Me₅Ir(H)₂(SiEt₃)₂ (1.594 (3) Å),[38] which to our knowledge are the only precise single-crystal neutron diffraction values reported to date. The terminal Pt–H bond distance in **4** is 1.610 (2) Å.[31]

The coordination around the metal centers is distorted significantly from the ideal geometry. Around the Ir atom, the angle involving HT1 and HT2 and that involving HB1 and HB2 are significantly smaller than 90° (76.99 (15) and 80.13 (12)°, respectively). The P1–Ir–P2 angle also is distorted significantly (168.91 (6)°), possibly due to steric repulsion between these phosphine ligands and L₂PtH₂. The Ir–P bond distance of 2.300 (2) Å is comparatively short, similar to that found in **14** (2.309 (1) Å)[37] and in the isolobal compound **5** (2.293 (2) Å),[22] but longer than in the presence of a mixed μ-Cl, μ-H bridge as in **6** (2.267 (4) Å), where a weaker metal–metal interaction is present (Rh–Ir = 2.899 (1) Å).[23] It may be noted that, when a terminal hydride (equatorial position) is substituted by a better donor ligand (e.g. PR₃), there is a significant lengthening of the Ir–P axial bond as

(32) Donohue, J. *The Structure of the Elements*; Wiley: New York, 1974.
(33) Mason, R.; Mingos, D. M. P. *J. Organomet. Chem.* **1973**, *50*, 53.
(34) Churchill, M. R.; Chang, S. W. Y. *Inorg. Chem.* **1974**, *13*, 2413.
(35) Shaik, S.; Hoffmann, R.; Fisel, C. R.; Summerville, R. H. *J. Am. Chem. Soc.* **1980**, *102*, 4555.

(36) Bau, R.; Teller, R. G.; Kirtley, S. W.; Koetzle, T. F. *Acc. Chem. Res.* **1979**, *12*, 176.
(37) Garlaschelli, L.; Khan, S. I.; Bau, R.; Longoni, G.; Koetzle, T. F. *J. Am. Chem. Soc.* **1985**, *107*, 7212.
(38) Ricci, J. S., Jr.; Koetzle, T. F.; Fernandez, M.-J.; Maitlis, P. M.; Green, J. C. *J. Organomet. Chem.* **1986**, *299*, 383.

Table IV. Bond Distances (Å) and Angles (deg) for Bimetallic Hydrio-Bridged Complexes[a]
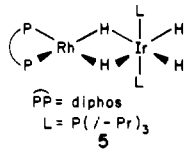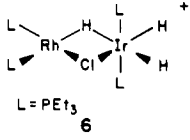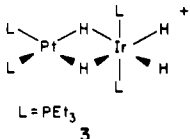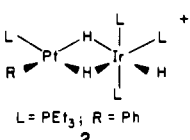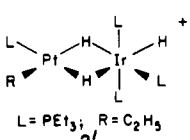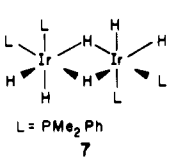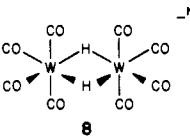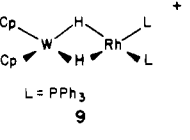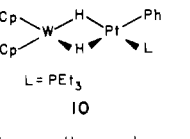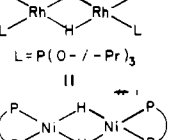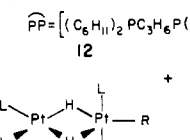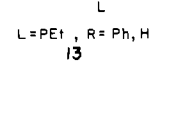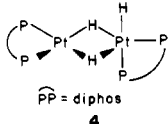
compd	M–M	M–P$_{ax}$	M–P$_{eq}$	M–H$_b$	M–H$_t$	M–H–M	method	ref
Rh–Ir, PP = diphos, L = P(i-Pr)$_3$ **5**	2.662 (1)	2.293 (2)	2.197 (2)				X	22
Rh–Ir, L = PEt$_3$ **6**	2.899 (1)	2.267 (4)[b]	2.243 (3)[c,d] 2.199 (3)				X	23
Pt–Ir, L = PEt$_3$ **3**	2.667 (1)	2.300 (3)[b]	2.275 (2)[e]	1.880 (3)[f] 1.731 (3)[g]	1.588 (3)	95.5 (1)	N	this work
Pt–Ir, L = PEt$_3$; R = Ph **2**	2.690 (1)	2.347 (5)[b]	2.224 (6)[g]				X	7
Pt–Ir, L = PEt$_3$; R = C$_2$H$_5$ **2′**	2.682 (1)	2.335 (4)[b]	2.224 (4)[g]				X	7
Ir–Ir, L = PMe$_2$Ph **7**	2.739 (1)	2.315 (3)	2.231 (3)	1.67 (6) 1.53 (7)	1.75 (7)		X	24
W–W (CO), **8**	3.010 (2)			1.920 (3) 1.933 (2)		102.7 (1)	N	25
Cp W–Rh, L = PPh$_3$ **9**	2.721 (8)						X	26
Cp W–Pt, L = PEt$_3$ **10**	2.663 (1)		2.216 (5)[g]				X	27
Rh–Rh, L = P(O-i-Pr)$_3$ **11**	2.647 (13)		2.171 (9)	1.808 (14)		94.1 (4)	N	28
Ni–Ni, PP = [(C$_6$H$_{11}$)$_2$PC$_3$H$_6$P(C$_6$H$_{11}$)$_2$] **12**	2.441 (1)			1.58 (4)		100	X	29
Pt–Pt—R, L = PEt$_3$, R = Ph, H **13**	2.819 (1)[i] 2.826 (2)[j]	2.292 (3)[i] 2.286 (6)	2.257 (3)[i] 2.269 (6) 2.289 (6)				X	30

Table IV (Continued)

compd	M-M	M-P$_{ax}$	M-P$_{eq}$	M-H$_b$	M-H$_t$	M-H-M	method	ref
 PP = diphos **4**	2.711 (1)	2.312 (1)	2.231 (1) 2.259 (1)^d 2.278 (1)^d	1.66–2.05^k	1.610 (2)	93.4–99.4^k	N	31

^{a} Key: ax = axial; eq = equatorial; b = bridging H; t = terminal H; diphos = Ph$_2$P(CH$_2$)$_2$PPh$_2$; X = X-ray diffraction, N = neutron diffraction. ^{a} M = Ir. ^{c} M = Rh. ^{d} P trans to H. ^{e} M = Pt. ^{f} M = Ir. ^{g} M = Pt. ^{h} As the PPN$^+$ salt. ^{i} Values referring to L = PEt$_3$, R = Ph. ^{j} Values referring to L = PEt$_3$, R = H. ^{k} Range of values.

in compounds **2** and **2'** (compared **2a** with **2b** and **2c**, or **2'a** with **2'b** and **2'c**) or in [(diphos)Rh(μ-H)(μ-Cl)Ir(H)(PEt$_3$)$_3$]$^+$ (**15**) (average 2.365 (6) Å)[39] and [(Ph$_3$P)Au(μ-H)Ir(H)$_2$(PPh$_3$)$_3$]$^+$ (2.397 (4) Å)[40] and this may be related to a difference in electron density on the metal center.[23]

The coordination around the Pt(II) also is appreciably distorted, as can be judged from the value of the HB1–Pt–HB2 and P3–Pt–P4 angles (88.70 (13) and 96.87 (6)°, respectively). The Pt–P bond distance (2.275 (2) Å) is as expected for an equatorial phosphine trans to a hydride. This bond length may be compared with that found when PR$_3$ is trans to a chlorine as in **6** (2.199 (4) Å),[23] in [(diphos)Rh(μ-H)(μ-Cl)IrCl(PEt$_3$)$_3$]$^+$ (**16**) (2.199 (3) Å),[39] and in **15** (2.213 (6) Å);[39] this lengthening is consistent with the bridging hydrides having a strong trans influence. We note however that the trans influence of the bridging hydride varies considerably with the strength of the hydrogen bridge, the H–M–L angle, and the presence of a mixed bridge. For example, in compounds **15** and **16** the bridging H and Cl atoms exert similar trans influences, as judged from the similar Rh–P bond lengths.[41,42] Moreover, these bond distances appear also to be related to the extent of the M–M interactions.[23]

It may be interesting to note that in **3** the M–M–P$_{eq}$ angles (i.e. Ir–Pt–P3 and Ir–Pt–P4) are very similar (131.73 (5) and 131.38 (6)°, respectively), an observation consistent with the M–H bond lengths being equal in pairs. In contrast, when distinct M–H distances are present in the bridge, as for example in **4**, the M–M–P angles differ (140.8 (4) and 132.6 (4)°). This observation may be used as an indication of the existence of an asymmetric bridge:[39,40] e.g., the Ir–Rh–P angles in compound **6** are 116.99 (8) and 145.11 (6)°, respectively, while in **15** the values 122.04 (9) and 155.09 (3)° are found.

On the basis of the "donor–acceptor" scheme, cation **3** can be considered to result from the coordination of the 16-electron species *cis*-[PtH$_2$(PEt$_3$)$_2$] with the 14-electron fragment {IrH$_2$(PEt$_3$)$_2$}$^+$. Thus, the Pt–H$_b$ distances are only approximately 0.1 Å longer than the value for Pt–H terminal bonds, while the Ir–H$_b$ distances are about 0.3 Å longer than those for the corresponding Ir–H$_t$ bonds (see Table III). The above representation is consistent with the chemistry of the {IrH$_2$(PR$_3$)$_2$}$^+$ fragment, easily obtained in the form of its disolvate [IrH$_2$(solv)$_2$L$_2$]$^+$.[43]

There are no unusually short intermolecular nonbonded contacts in the crystal structure of **3**. The intramolecular separation be-

tween hydrides HT1 and HT2 is 1.977 (4) Å; this distance is in the range expected from the values found in polyhydrido complexes.[44] It may also be worthy of note that the H$_b$···H$_b$ distances in M(μ-H)$_2$M compounds are fairly constant at about 2.4 Å[25] (viz., in **3**, 2.421 (4) Å).

The geometry of the [BPh$_4$]$^-$ anion is worthy of comment. A complete list of bond distances and angles and a drawing are included in the supplementary material (Table S5(b) and Figure S1). The B atom is in a distorted-tetrahedral environment (C–B–C angles in the range 107.8 (1)–112.7 (1)°, average 109.5 (1.0)°) with one B–C bond slightly longer than the others (average 1.663 (2) and 1.650 (1) Å, respectively). The geometries of the four phenyl rings are indistinguishable, but a pronounced distortion is present, lowering their symmetry to C$_{2v}$. Such systematic distortions of phenyl rings have been attributed to the presence of substitutents on the rings,[45] as discussed previously.[45-47] In particular, the change of the ipso angle (α)[48] is found to be linearly dependent on the electronegativity of the substituent, while a more complex pattern of distortions may affect the other angles.[47] Here we note that the low-electronegativity substitutent, boron, causes the expected decrease in the value of the α angle (average 115.4 (1)°); the β and δ angles are also affected (average values 122.6 (1) and 118.7 (1)°, respectively) while γ retains the ideal sp^2 value (average 120.3 (1)°). A much smaller effect of the substitutent on bond lengths is also noticeable,[45] the longest bond (a) being 1.410 (1) Å (average value) and the shortest (c) 1.395 (1) Å (average value).

Supplementary Material Available: Atomic positional and thermal parameters from the X-ray (Table S1) and neutron (Table S3) analyses, an extensive list of bond distances and angles (Table S5), and a view of the [BPh$_4$]$^-$ anion (Figure S1) (19 pages); observed and calculated structure factors (Table S2, X-ray; Table S4, neutron) (98 pages). Ordering information is given on any current masthead page.

(39) Lehner, M.; Matt, D.; Togni, A.; Thouvenot, R.; Venanzi, L. M.; Albinati, A. *Inorg. Chem.* **1984**, *23*, 4254.

(40) Lehner, H.; Matt, D.; Pregosin, P. S.; Venanzi, L. M.; Albinati, A. *J. Am. Chem. Soc.* **1983**, *104*, 1825.

(41) Appleton, T. G.; Clark, H. C.; Manzer, L. E. *Coord. Chem. Rev.* **1973**, *10*, 335.

(42) Brown, M. P.; Puddephatt, R. J.; Rashidi, M.; Seddon, K. R. *J. Chem. Soc., Dalton Trans.* **1978**, 516.

(43) Crabtree, R. H.; Demon, P. C.; Eden, D.; Mihelcic, J. M.; Parnell, C. A.; Quirk, J. M.; Morris, G. E. *J. Am. Chem. Soc.* **1982**, *104*, 6994.

(44) Teller, R. G.; Bau, R. *Struct. Bonding (Berlin)* **1981**, *44*, 1.

(45) Domenicano, A.; Vaciago, A.; Coulson, C. A. *Acta Crystallogr., Sect. B: Struct. Crystallogr. Cryst. Chem.* **1975**, *B31*, 221.

(46) Norrestam, R.; Schepper, L. *Acta Chem. Scand., Ser. A* **1981**, *A35*, 91.

(47) Domenicano, A.; Murray-Rust, P.; Vaciago, A. *Acta Crystallogr., Sect. B: Struct. Sci.* **1983**, *B39*, 457 and references cited therein.

(48) The nomenclature is taken from ref 47, viz.

X = B